

Enhancement of Opto-Electro-Mechanical Entanglement through Three-Level Atoms

Abebe Senbeto Kussia^a, Tewodros Yirgashewa Darge^b, Tesfay Gebremariam Tesfahannes^c, Abeba Teklie Bimeraw^c, Berihu Teklu^d

^aCollege of Natural Science, Department of Physics, Salale University, Fitcha, 245, Ethiopia,

^bCollege of Natural Science, Department of Applied Physics, Adama Science and Technology University, Adama, 1888, Ethiopia

^cCollege of Natural Science, Department of Physics, Arba Minch University, Arba Minch, 21, Ethiopia

^dCollege of Computing and Mathematical Sciences, Department of Mathematics, Khalifa University of Science and Technology, Khalifa, 127788, Abu Dhabi, United Arab Emirates

Abstract

We address the dynamical bipartite entanglement in an opto-electro-mechanical system that involves a three-level atom. The system consists of a degenerate three-level atom, a mechanical resonator, an optical cavity, and a microwave cavity. By utilizing the linearization approximation and nonlinear quantum-Langevin equations, the dynamics of the system are analyzed, and the bipartite entanglement is evaluated using the logarithmic negativity. The research findings indicate that the entanglement between each subsystem increases with the atom injection rate, suggesting that a higher atom injection rate leads to enhanced information transmission between the subsystems. Additionally, it is observed that the correlation between subsystems increases with an increase in the coupling rate. Moreover, the study demonstrates that the correlation between each subsystem decreases as temperature rises. The results highlight the positive impact of three-level atoms on the bipartite entanglement in an opto-electro-mechanical system. Consequently, such electro-optomechanical systems can offer a framework for optomechanical information transfer.

Keywords: Opto-electro-mechanical system, Degenerate three-level atom, Linearization approximation, Entanglement.

1. Introduction

Over the past few decades, cavity optomechanics, which investigates the nonlinear interaction through radiation-pressure force, has made significant progress in both experimental and theoretical domains [1, 2, 3, 4, 5]. Numerous research on optomechanical systems have been fascinating such as cooling ground state [6, 7], feedback cooling [8], normal mode splitting [9] and two-mode squeezed states [10]. Progress in those diverse optomechanical devices has been developed to perform and enhance the nonlinear quantum phenomena such as quantum entanglement [11, 12, 13, 14], high precision metrology [15, 16, 17, 18], optomechanical storage [19] and quantum information processing [20]. In quantum information processing, quantum entanglement is an important quantum mechanics phenomenon and plays a significant role in processes such as quantum teleportation [21], quantum key distribution [22], population transfer [23], quantum secure direct communication [24, 25, 26] and quantum state sharing [27].

Among these researches, intracavity entanglement is attainable with a coherent two-mode squeezing interaction, and steady-state entanglement is achieved in a three-mode optomechanical system [28]. Furthermore, the optomechanical dark mode successfully achieved by weakly coupling [29, 30], multimode circuit optomechanical systems may be used in the interconversion of microwave and optical photons [31, 32]. Such hybrid systems may allow to improve microwave quantum illumination

[33] and to realize an information transfer between an optical and microwave cavity modes [34]. On the other hand, the nonlinear interaction of a three-level atom with a two-mode field in an optomechanical cavity enhances the non-classical properties through nonlinear atom-field coupling [35]. However, an optomechanical system with two-level and three-level atoms has been studied and has many potential applications.

The study of nano-opto-electro-mechanical systems has made remarkable strides recently, paving the way for significant advancements in this discipline and offering excellent opportunities to control light flow in nano-photonics structures [36]. Among these, opto-electro-mechanical systems have gained considerable interest due to their potential applications in theoretical and experimental frameworks. A notable example of such advancements is the work by [37], which demonstrates the generation of EPR-entangled states between optical and mechanical modes. This study showcases the dynamical entanglement and quantum steering within a pulsed hybrid opto-electro-mechanical system, highlighting the intricate interplay between different physical domains to achieve quantum control and manipulation. They propose that the mechanical oscillator performs better and more efficiently in connecting microwave and optical modes of the electromagnetic spectrum. Furthermore, Li et al. [36] have proposed an experimental demonstration of entanglement between a mechanical resonator and a microwave LC resonator in opto-electro-mechanics. This electro-mechanical coupling serves as the source entanglement, which can exist in a stationary state and is temperature-resistant. Recent advancements in the nano-opto-electro mechanical sys-

Email address: tesfaye.gbremariam@amu.edu.et (Tesfay Gebremariam Tesfahannes)

tems offer a foundation for further research in this area and excellent opportunities to control the flow of light in nanophotonic structures [38]. Additionally, Cattiaux et al. [39] present the nonlinear dynamics of microwave optomechanics in the classical regime, suggesting that coupling optical fields to microwave signals through a mechanical resonator holds significant promise for both current and future quantum information technologies.

Moreover, the potential of the opto-electro-mechanics systems to produce the stationary entanglement dynamics between the subsystems have been investigated in [40]. In their study, the mechanical resonator simultaneously coupled to both microwave and optical cavities through a capacitor plate coupling process. Consequently, such cavity electro-mechanical systems have gained interest as potential contender for microwave-based photonic devices. Furthermore, many schemes have been proposed to generate entanglement in nano-electro-optomechanical systems[41, 42] and in various systems[43, 44].

Recently, Pan et al. studied the entanglement phenomena using an electro-optical hybrid system that included an optical parametric amplifier and a Coulomb force interaction. They hypothesized that the two charged oscillators improved the entanglement and output squeezing in the hybrid system. The enhancement of bipartite entanglement in nano-electro-optomechanical systems, especially in the presence of three-level atoms, remains an active area of research.

In this paper, we theoretically investigate dynamical bipartite entanglement in an opto-electro-mechanical system through the incorporation of a three-level atom. We examine a model in which a degenerate three-level atom is injected into the optical cavity at a constant rate. A three-level atom's upper, middle, and lower levels are labeled in a cascade configuration. The main advantage of incorporating a three-level atom into an opto-electro-mechanical system is to improve the bipartite entanglement between the subsystems under strong coupling. Moreover, the presence of the three-level atom facilitates effective state transfer and information manipulation between the subsystems. We examine the enhancement of the bipartite entanglement through logarithmic negativity. Compared to a scheme without the presence of a three-level atom, the incorporation of a three-level atom provides several advantages, such as enhancing the possibilities for bipartite entanglement. Our findings indicate that the entanglement between the optical cavity and the three-level atom, as well as normalized optical cavity detuning, increases with a higher coupling rate. Additionally, as the atom injection rate rises, the entanglement between each subsystem grows since a higher atom injection rate results in increased laser emission.

2. Model and Hamiltonian Formulation

In this paper, we consider a model of opto-electro-mechanical system in which a degenerate three level atom is injected into a cavity at constant rate r_a as shown in Fig. (1). In a cascade configuration, we label the top, intermediate, and

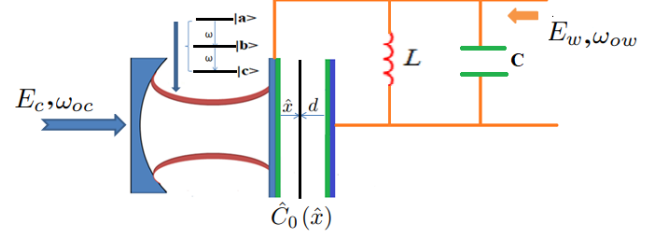


Figure 1: Schematic diagram of hybrid opto-electro-mechanical system with degenerate three-level atom.

bottom levels of a three-level atom as $|a\rangle$, $|b\rangle$ and $|c\rangle$, respectively. When the atom makes a transition from the upper to the intermediate level and then from the intermediate to the bottom level, two photon modes with the same frequency are emitted [45]. We assume the transitions between levels $|a\rangle$ and $|b\rangle$ and between levels $|b\rangle$ and $|c\rangle$ to be dipole allowed, with the direct transition between levels $|a\rangle$ and $|c\rangle$ being dipole forbidden. Additionally, we assume a mechanical resonator (MR) that is linked to a driven optical cavity (OC) with a resonance frequency of ω_c and, on the other side, capacitively connected to the field of a superconducting microwave cavity (MC) of ω_w .

To describe the dynamics of the system, we employ the Hamiltonian formalism. The total Hamiltonian H of the system can be written as the sum of the Hamiltonians of the individual components and their interactions [46]:

$$\begin{aligned} \hat{H} = & \frac{\hat{p}_x^2}{2m} + \frac{m\omega_m^2 \hat{x}^2}{2} + \frac{\hat{\Phi}^2}{2L} + \frac{\hat{Q}^2}{2[C + \hat{C}_o(\hat{x})]} - e(t)\hat{Q} \\ & + \hbar\omega_c \hat{a}^\dagger \hat{a} + \sum_{i=a,b,c} \hbar E_i \hat{\sigma}_{ii} - \hbar G_{oc} \hat{a}^\dagger \hat{a} \hat{x} + \hbar g(\hat{\sigma}_{ba} \hat{a}^\dagger \\ & + \hat{\sigma}_{cb} \hat{a}^\dagger + \hat{a} \hat{\sigma}_{ab} + \hat{a} \hat{\sigma}_{bc}) + i\hbar E_c (\hat{a}^\dagger e^{-i\omega_{oc}t} - \hat{a} e^{i\omega_{oc}t}), \end{aligned} \quad (1)$$

where (\hat{x}, \hat{p}_x) represent the canonical position and momentum of a MR with frequency ω_m and commutation relation $[\hat{x}, \hat{p}_x] = i\hbar$, $(\hat{\Phi}, \hat{Q})$ represent the canonical coordinates of the MC with the commutation relation $[\hat{Q}, \hat{\Phi}] = i\hbar$, describing the flux through an equivalent inductor L and the charge on an equivalent capacitor C , respectively. $G_{oc} = (\frac{\omega_c}{\ell}) \sqrt{\frac{\hbar}{m\omega_m}}$ is the optomechanical coupling rate with m the effective mass of mechanical mode, and ℓ the length of the optical Fabry-Perot cavity. The coherent driving of the microwave cavity (MC) with damping rate κ_w is given by:

$$e(t) = -i\sqrt{2\hbar\omega_w L} E_w (e^{i\omega_{ow}t} - e^{-i\omega_{ow}t}). \quad (2)$$

The microwave resonator is driven by a tunable electric field, which acts as a control part of the system and interacts with the

cavity field through the mediator of MR [47]. The microwave cavity and the MR are coupled because the microwave cavity's capacity depends on the resonator displacement, C_o . This function is expanded around the resonator's equilibrium position, which corresponds to the separation d between the capacitor's plates and a corresponding bare capacitance of C_o . Expanding $\hat{C}_o(\hat{x}) = C_o[\frac{1+\hat{x}(t)}{d}]$ and using a Taylor series for the capacitive energy, we find to first order:

$$\frac{\hat{Q}^2}{2[C + \hat{C}_o(\hat{x})]} = \frac{\hat{Q}^2}{2C_\Sigma} - \frac{\mu}{2dC_\Sigma} \hat{x}(t) \hat{Q}^2, \quad (3)$$

where $C_\Sigma = C + C_o$ and $\mu = \frac{C_o}{C_\Sigma}$ [48]. Using this expression, the Hamiltonian of Eq. (1) can be rewritten in the terms of the raising and lowering operators of the MC field \hat{b}, \hat{b}^\dagger where $[\hat{b}, \hat{b}^\dagger] = 1$ and the dimensionless position and momentum operators of the MR, \hat{q}, \hat{p} where $[\hat{q}, \hat{p}] = i\hbar$ as

$$H = \hbar\omega_w \hat{b}^\dagger \hat{b} + \hbar\omega_c \hat{a}^\dagger \hat{a} + \sum_{i=a,b,c} \hbar E_i \hat{\sigma}_{ii} + \frac{\hbar\omega_m}{2} (\hat{p}^2 + \hat{q}^2) - \frac{\hbar G_{ow}}{2} \hat{q} (\hat{b} + \hat{b}^\dagger)^2 - \hbar G_{oc} \hat{q} \hat{a}^\dagger \hat{a} - i\hbar E_w (e^{i\omega_{ow}t} - e^{-i\omega_{ow}t}) (\hat{b} + \hat{b}^\dagger) + i\hbar E_c (\hat{a}^\dagger e^{-i\omega_{oc}t} - \hat{a} e^{i\omega_{oc}t}) + \hbar g (\hat{\sigma}_{ba} \hat{a}^\dagger + \hat{\sigma}_{cb} \hat{a}^\dagger + \hat{a} \hat{\sigma}_{ab} + \hat{a} \hat{\sigma}_{bc}), \quad (4)$$

where $\hat{b} = \frac{L\omega_w \hat{Q} + i\hat{\Phi}}{\sqrt{2L\hbar\omega_w}}$, $\hat{q} = \sqrt{\frac{m\omega_m}{\hbar}} \hat{x}$, and $G_{ow} = \frac{\mu\omega_w}{2d} \sqrt{\frac{\hbar}{m\omega_m}}$. To obtain the standard Hamiltonian of the system in terms of microwave, optical, and atom detuning, we first apply the rotating wave approximation (RWA) on Eq. (4) to eliminate fast oscillating terms [49]. The RWA assumes that the slowly varying terms of the Hamiltonian have a significant contribution to the dynamics, while the rapidly oscillating terms do not. Thus, the final Hamiltonian of the system becomes:

$$\hat{H} = \hbar\Delta_{ow} \hat{b}^\dagger \hat{b} + \hbar\Delta_{oc} \hat{a}^\dagger \hat{a} + \hbar\Delta_{a1} \hat{\sigma}_{aa} + \hbar\Delta_{a2} \hat{\sigma}_{cc} + \frac{\hbar\omega_m}{2} (\hat{p}^2 + \hat{q}^2) - \hbar G_{ow} \hat{q} \hat{b}^\dagger \hat{b} - \hbar G_{oc} \hat{q} \hat{a}^\dagger \hat{a} - i\hbar E_w (\hat{b} - \hat{b}^\dagger) + i\hbar E_c (\hat{a}^\dagger - \hat{a}) + \hbar g (\hat{\sigma}_{ba} \hat{a}^\dagger + \hat{\sigma}_{cb} \hat{a}^\dagger + \hat{a} \hat{\sigma}_{ab} + \hat{a} \hat{\sigma}_{bc}). \quad (5)$$

where $\Delta_{ow} = \omega_w - \omega_{ow}$ is the microwave detuning with deriving frequency, $\Delta_{oc} = \omega_c - \omega_{oc}$ is optical cavity detuning, $\Delta_{a1} = \omega - \omega_{oc}$ and $\Delta_{a2} = \omega - \omega_{oc}$ are the detunings between atomic transition frequencies and driving laser frequency, with ω being the atomic transition frequencies. The last term describes the coupling between cavity mode and the three level atom with interaction strength g .

3. Dynamics of the system

The dynamics of an opto-electro-mechanical system assisted by three-level atoms can be described by a set of nonlinear quantum Langevin equations (QLEs), which incorporate both dissipation and fluctuation terms. These equations are derived from the Heisenberg equations of motion for the system operators, with additional terms representing the interaction with

the environment. To obtain the nonlinear dynamics of the system operators $\hat{q}, \hat{p}, \hat{a}, \hat{b}, \hat{\sigma}_{ba}$ and $\hat{\sigma}_{cb}$, we use the Langevin-Heisenberg equation of motion (QLEs). Setting $\hbar = 1$, the QLEs for the system operators can be written as follows:

$$\begin{aligned} \dot{\hat{q}} &= \omega_m \hat{p}, \\ \dot{\hat{p}} &= -\omega_m \hat{q} + \hbar G_{ow} \hat{b}^\dagger \hat{b} + \hbar G_{oc} \hat{a}^\dagger \hat{a} - \gamma_m \hat{p} + \xi, \\ \dot{\hat{a}} &= -(\kappa_c + \Delta_{oc}) \hat{a} + iG_{oc} \hat{q} \hat{a} + E_c - ig(\hat{\sigma}_{ba} + \hat{\sigma}_{cb}) + \sqrt{2\kappa_c} \hat{a}^{in}, \\ \dot{\hat{b}} &= -(\kappa_w + \Delta_{ow}) \hat{b} + iG_{ow} \hat{q} \hat{b} + E_w + \sqrt{2\kappa_w} \hat{b}^{in}, \\ \dot{\hat{\sigma}}_{ba} &= -(\kappa_a + i\Delta_{a1}) \hat{\sigma}_{ba} + ig \hat{\sigma}_{ca} \hat{a}^\dagger - ig \hat{a} (\hat{\sigma}_{bb} - \hat{\sigma}_{aa}) + \sqrt{2\kappa_a} \hat{\sigma}_{ba}^{in}, \\ \dot{\hat{\sigma}}_{cb} &= -(\kappa_a - i\Delta_{a2}) \hat{\sigma}_{cb} - ig \hat{\sigma}_{ca} \hat{a}^\dagger - ig \hat{a} (\hat{\sigma}_{cc} - \hat{\sigma}_{bb}) + \sqrt{2\kappa_a} \hat{\sigma}_{cb}^{in}, \end{aligned} \quad (6)$$

where $\gamma_m, \kappa_c, \kappa_w$ are mechanical damping rate, cavity decay rate and microwave cavity decay rate respectively. The random Brownian stochastic force $\xi(t)$ acting on the mechanical mode affects the mechanical resonator and it is coupled to a thermal bath at a damping rate of γ_m with the correlation function [50] The optical and microwave cavity amplitude decay at a rate κ_c and κ_w is affected by the radiation input noise $a^{in}(t)$ and $b^{in}(t)$ whose correlation function given by [51]

$\langle \hat{a}^{in}(t) \hat{a}^{in\dagger}(t') \rangle = [N(\omega_c) + 1] \delta(t - t')$, $\langle \hat{b}^{in}(t) \hat{b}^{in\dagger}(t') \rangle = [N(\omega_w) + 1] \delta(t - t')$, $\langle \hat{b}^{in\dagger}(t) \hat{b}^{in}(t') \rangle = N(\omega_w) \delta(t - t')$, where $N(\omega_c) = [\exp(\hbar\omega_c/\kappa_B T) - 1]^{-1}$ and $N(\omega_w) = [\exp(\hbar\omega_w/\kappa_B T) - 1]^{-1}$ are the equilibrium mean thermal photon numbers of the optical and microwave fields respectively. One can safely assume $N(\omega_c) \approx 0$ since $\hbar\omega_c/\kappa_B T \gg 1$ at optical frequencies, while thermal microwave photons cannot be neglected in general, even at very low temperatures. The correlation function of atomic input noise operators depends on the specifics of the system under consideration. In our case we assume that the correlation function of atomic input noise operators is considered as Markovian Gaussian noise, meaning it only depends on the current state and has no memory of past states which is described by delta function as $\langle \hat{\sigma}_{ba}^{in}(t) \hat{\sigma}_{ab}^{in\dagger}(t') \rangle = [N(\omega) + 1] \delta(t - t')$, $\langle \hat{\sigma}_{ab}^{in}(t) \hat{\sigma}_{ba}^{in\dagger}(t') \rangle = N(\omega) \delta(t - t')$, $\langle \hat{\sigma}_{cb}^{in}(t) \hat{\sigma}_{bc}^{in\dagger}(t') \rangle = [N(\omega) + 1] \delta(t - t')$, $\langle \hat{\sigma}_{bc}^{in}(t) \hat{\sigma}_{cb}^{in\dagger}(t') \rangle = N(\omega) \delta(t - t')$, where $N(\omega) = [\exp(\hbar\omega/\kappa_B T) - 1]^{-1}$ and $N(\omega) = [\exp(\hbar\omega/\kappa_B T) - 1]^{-1}$. We assuming that the initial state of a three-level atom $\rho_a = \rho_{aa}^0 |a\rangle \langle a| + \rho_{cc}^0 |c\rangle \langle c| + \rho_{ca}^0 (|c\rangle \langle a| + |a\rangle \langle c|)$ to be injected in to the cavity at constant rate of r_a [52]. As the result we can rewrite the last two equations of Eq. (6) as

$$\dot{\hat{\sigma}}_{ba} = -(\kappa_a + i\Delta_{a1}) \hat{\sigma}_{ba} + ig r_a \rho_{ca}^0 \hat{a}^\dagger + ig r_a \rho_{aa}^0 \hat{a} + \sqrt{2\kappa_a} \hat{\sigma}_{ba}^{in}, \quad (7)$$

$$\dot{\hat{\sigma}}_{cb} = -(\kappa_a - i\Delta_{a2}) \hat{\sigma}_{cb} - ig r_a \rho_{ca}^0 \hat{a}^\dagger - ig r_a \rho_{cc}^0 \hat{a} + \sqrt{2\kappa_a} \hat{\sigma}_{cb}^{in}. \quad (8)$$

The dynamics of open quantum systems in interaction with a reservoir, which is typically modeled as a collection of harmonic oscillators that are linearly coupled to the system. The linearization of the above nonlinear Quantum Langevin equations of the system operators is done by assuming that the light mode is strongly driven leading to the amplitude of its mean value $|\alpha_s| \gg 1$. This allows us to linearize the dynamics of our system around the steady-state values by expanding our system operators $\hat{q}, \hat{p}, \hat{a}, \hat{b}, \hat{\sigma}_{ba}$, and $\hat{\sigma}_{cb}$ as a sum of its coherent ampli-

tudes semi classical steady-state value plus an additional small fluctuation operator with zero mean values [53].

3.1. Steady State Solutions of the Equations of Motion

The steady state solution of the system refers to finding a stable equilibrium condition in which the opto-electro-mechanical system exhibits constant behavior over time, with no net changes in dynamic parameters. The steady state solution is critical for understanding the system's long-term behavior, stability, and performance. To obtain the steady state solution of the system operators, we set the time derivatives to zero and calculate the mean values of the operators. The steady state does not fluctuate with time. Using the Langevin equations from Eqs. (6) and Eqs. (7)-(8), and noting that the mean values of the input noise terms and fluctuation terms are zero, the steady state solutions of the system operators become:

$$\begin{aligned} p_s &= 0, \quad q_s = \frac{G_{oc}|\alpha_s|^2 + G_{ow}|\beta_s|^2}{\omega_m}, \\ \alpha_s &= \frac{E_c - ig(\sigma_{ba_s} + \sigma_{cb_s})}{i\Delta_c + \kappa_c}, \quad \beta_s = \frac{E_w}{i\Delta_w + \kappa_w}, \\ \sigma_{ba_s} &= \frac{igr_a(\rho_{ca}^0 + \rho_{aa}^0)}{\kappa_a + i\Delta_{a1}}\alpha_s, \quad \sigma_{cb_s} = -\frac{igr_a(\rho_{ca}^0 + \rho_{cc}^0)}{\kappa_a - i\Delta_{a2}}\alpha_s, \end{aligned} \quad (9)$$

where $\Delta_c = \Delta_{oc} - G_{oc}q_s$ and $\Delta_w = \Delta_{ow} - G_{ow}q_s$ describe the effective detuning of the optical and microwave cavities field respectively. The dynamics of the fluctuation of the operators in the system is obtained by decomposing each operators as a sum of its steady-state value and a small fluctuation. The fluctuation of the operators of the system is obtained by Eqs. (6) and Eqs. (7)-(8) and neglect the second order fluctuations (small terms), $\delta\hat{q}\delta\hat{a} \approx \delta\hat{q}\delta\hat{b} \approx \delta\hat{q}\delta\hat{a}^\dagger \approx \delta\hat{q}\delta\hat{b}^\dagger \approx 0$. The fluctuation of the system operators can be written as:

$$\begin{aligned} \delta\hat{q} &= \omega_m\delta\hat{p}, \\ \delta\hat{p} &= -\omega_m\delta\hat{q} - \gamma_m\delta\hat{p} + G_{oc}\alpha_s(\delta\hat{a}^\dagger + \delta\hat{a}) + G_{ow}\beta_s(\delta\hat{b}^\dagger + \delta\hat{b}) + \xi, \\ \delta\hat{a} &= -(i\Delta_c + \kappa_c)\delta\hat{a} + iG_{oc}\alpha_s\delta\hat{q} - ig(\delta\hat{\sigma}_{ba} + \delta\hat{\sigma}_{cb}) + \sqrt{2\kappa_c}\hat{a}^{in}, \\ \delta\hat{b} &= -(i\Delta_w + \kappa_w)\delta\hat{b} + iG_{ow}\beta_s\delta\hat{q} + \sqrt{2\kappa_w}\hat{b}^{in}, \\ \delta\hat{\sigma}_{ba} &= -(\kappa_a + i\Delta_{a1})\delta\hat{\sigma}_{ba} + igr_a\rho_{ca}^0\hat{a}^\dagger + igr_a\rho_{aa}^0\hat{a} + \sqrt{2\kappa_a}\hat{\sigma}_{ba}^{in}, \\ \delta\hat{\sigma}_{cb} &= -(\kappa_a - i\Delta_{a2})\delta\hat{\sigma}_{cb} - igr_a\rho_{ca}^0\hat{a}^\dagger - igr_a\rho_{cc}^0\hat{a} + \sqrt{2\kappa_a}\hat{\sigma}_{cb}^{in}, \end{aligned} \quad (10)$$

where α_s and β_s are real and positive the chosen phase reference for the optical and microwave field.

3.2. The quantum fluctuations and covariance matrix of the system

In order to study the entanglement properties of opto-electro-mechanical systems the quantum correlations between appropriate quadratures of the two intracavity fields and the position

and momentum of the resonator are studied. Hence we introduce the dimensionless quadrature fluctuation for each system operator. The optical cavity field fluctuation quadratures

$\delta\hat{X}_c = \frac{(\delta\hat{a} + \delta\hat{a}^\dagger)}{\sqrt{2}}, \delta\hat{Y}_c = \frac{(\delta\hat{a} - \delta\hat{a}^\dagger)}{i\sqrt{2}}, \delta\hat{X}_w = \frac{(\delta\hat{b} + \delta\hat{b}^\dagger)}{\sqrt{2}}, \delta\hat{Y}_w = \frac{(\delta\hat{b} - \delta\hat{b}^\dagger)}{i\sqrt{2}}$, and the microwave cavity field fluctuation quadratures $\delta\hat{X}_{a_1} = \frac{(\delta\hat{\sigma}_{ba} + \delta\hat{\sigma}_{ab})}{\sqrt{2}}, \delta\hat{Y}_{a_1} = \frac{(\delta\hat{\sigma}_{ba} - \delta\hat{\sigma}_{ab})}{i\sqrt{2}}, \delta\hat{X}_{a_2} = \frac{(\delta\hat{\sigma}_{cb} + \delta\hat{\sigma}_{bc})}{\sqrt{2}}, \delta\hat{Y}_{a_2} = \frac{(\delta\hat{\sigma}_{cb} - \delta\hat{\sigma}_{bc})}{i\sqrt{2}}$. Using the above equations the linearized QLEs describing the system quadrature fluctuations for our proposed model becomes

$$\begin{aligned} \delta\dot{\hat{q}} &= \omega_m\delta\hat{p}, \\ \delta\dot{\hat{p}} &= -\omega_m\delta\hat{q} - \gamma_m\delta\hat{p} + G_c\delta\hat{X}_c + G_w\delta\hat{X}_w + \xi, \\ \delta\dot{\hat{X}}_c &= -\kappa_c\delta\hat{X}_c + \Delta_c\delta\hat{Y}_c + g\delta\hat{Y}_{a_1} + \delta\hat{Y}_{a_2} + \sqrt{2\kappa_c}\hat{X}_c^{in}, \\ \delta\dot{\hat{Y}}_c &= G_c\delta\hat{q} - \Delta_c\delta\hat{X}_c - \kappa_c\delta\hat{Y}_c - g\delta\hat{X}_{a_1} - g\delta\hat{X}_{a_2} + \sqrt{2\kappa_c}\hat{Y}_c^{in}, \\ \delta\dot{\hat{X}}_w &= -\kappa_w\delta\hat{X}_w + \Delta_w\delta\hat{Y}_w + \sqrt{2\kappa_w}\hat{X}_w^{in}, \\ \delta\dot{\hat{Y}}_w &= G_w\delta\hat{q} - \Delta_w\delta\hat{X}_w - \kappa_w\delta\hat{Y}_w + \sqrt{2\kappa_w}\hat{Y}_w^{in}, \\ \delta\dot{\hat{X}}_{a_1} &= gr_a(\rho_{ca}^0 - \rho_{aa}^0)\delta\hat{Y}_c - \kappa_a\delta\hat{X}_{a_1} + \Delta_{a1}\delta\hat{Y}_{a_1} + \sqrt{2\kappa_a}\hat{X}_{a_1}^{in}, \\ \delta\dot{\hat{Y}}_{a_1} &= gr_a(\rho_{ca}^0 + \rho_{aa}^0)\delta\hat{X}_c - \Delta_{a1}\delta\hat{X}_{a_1} - \kappa_a\delta\hat{Y}_{a_1} + \sqrt{2\kappa_a}\hat{Y}_{a_1}^{in}, \\ \delta\dot{\hat{X}}_{a_2} &= gr_a(\rho_{cc}^0 - \rho_{ca}^0)\delta\hat{Y}_c - \kappa_a\delta\hat{X}_{a_2} - \Delta_{a2}\delta\hat{Y}_{a_2} + \sqrt{2\kappa_a}\hat{X}_{a_2}^{in}, \\ \delta\dot{\hat{Y}}_{a_2} &= gr_a(\rho_{ca}^0 + \rho_{cc}^0)\delta\hat{X}_c + \Delta_{a2}\delta\hat{X}_{a_2} - \kappa_a\delta\hat{Y}_{a_2} + \sqrt{2\kappa_a}\hat{Y}_{a_2}^{in}, \end{aligned} \quad (11)$$

where $G_c = \sqrt{2}G_{oc}\alpha_s = \frac{\omega_c}{\ell} \sqrt{\frac{2\hbar}{m\omega_m}} \left[\frac{E_c - ig(\sigma_{ba_s} + \sigma_{cb_s})}{\kappa_c + i\Delta_c} \right]$ and $G_w = \sqrt{2}G_{ow}\beta_s = \frac{\mu\omega_w}{d} \sqrt{\frac{P_w\kappa_w}{m\omega_m\omega_{ow}(\kappa_w^2 + \Delta_w^2)}}$.

Eq. (11) can be written in the following covariance matrix form [54]

$$\dot{u}(t) = Au(t) + n(t). \quad (12)$$

The steady-state dynamics of the covariance matrix for an opto-electro-mechanical system is concerned with understanding how the statistical properties of the system reach equilibrium over time. Analyzing the covariance matrix provides insights into the correlations and entanglement between different parts of the OMEMS, which are crucial for understanding its quantum behavior, performance, and potential applications. Eq. (12) can be also written in matrix form as:

where $u(t) = (\delta\hat{q}(t), \delta\hat{p}(t), \delta\hat{X}_c(t), \delta\hat{Y}_c(t), \delta\hat{X}_w(t), \delta\hat{Y}_w(t), \delta\hat{X}_{a_1}(t), \delta\hat{Y}_{a_1}(t), \delta\hat{X}_{a_2}(t), \delta\hat{Y}_{a_2}(t))^T$, is quadrature fluctuation vector, $n(t) = (0, \xi(t), \sqrt{2\kappa_c}\hat{X}_c^{in}(t), \sqrt{2\kappa_c}\hat{Y}_c^{in}(t), \sqrt{2\kappa_w}\hat{X}_w^{in}(t), \sqrt{2\kappa_w}\hat{Y}_w^{in}(t), \sqrt{2\kappa_a}\hat{X}_{a_1}^{in}(t), \sqrt{2\kappa_a}\hat{Y}_{a_1}^{in}(t), \sqrt{2\kappa_a}\hat{X}_{a_2}^{in}(t), \sqrt{2\kappa_a}\hat{Y}_{a_2}^{in}(t))^T$ is the noise vector with the exponent T represent the transpose and A is the drift matrix (contains information about the system) and is given by

$$A = \begin{pmatrix} 0 & \omega_m & 0 & 0 & 0 & 0 & 0 & 0 & 0 & 0 \\ -\omega_m & -\gamma_m & G_c & 0 & G_w & 0 & 0 & 0 & 0 & 0 \\ 0 & 0 & -\kappa_c & \Delta_c & 0 & 0 & 0 & g & 0 & g \\ G_c & 0 & -\Delta_c & -\kappa_c & 0 & 0 & -g & 0 & -g & 0 \\ 0 & 0 & 0 & 0 & -\kappa_w & \Delta_w & 0 & 0 & 0 & 0 \\ G_w & 0 & 0 & 0 & -\Delta_w & -\kappa_w & 0 & 0 & 0 & 0 \\ 0 & 0 & 0 & gr_a(\rho_{ca}^0 - \rho_{aa}^0) & 0 & 0 & -\kappa_a & \Delta_{a1} & 0 & 0 \\ 0 & 0 & gr_a(\rho_{ca}^0 + \rho_{aa}^0) & 0 & 0 & 0 & -\Delta_{a1} & -\kappa_a & 0 & 0 \\ 0 & 0 & 0 & gr_a(\rho_{cc}^0 - \rho_{ca}^0) & 0 & 0 & 0 & 0 & -\kappa_a & -\Delta_{a2} \\ 0 & 0 & gr_a(\rho_{cc}^0 + \rho_{ca}^0) & 0 & 0 & 0 & 0 & 0 & \Delta_{a2} & -\kappa_a \end{pmatrix}. \quad (13)$$

Due to the linearized dynamics and the Gaussian nature of the quantum noises in Eq. (12), the steady state of the quantum fluctuations of the system is a continuous variable bipartite Gaussian state, which is completely characterized by the 10×10 correlation matrix V with its entries are defined as [55]: $V_{ij} = \frac{1}{2} \langle u_i(t)u_j(t') + u_j(t')u_i(t) \rangle$, where $(i, j = 1, 2, \dots, 10)$. Eq. (12) can be written in compact form as $\dot{u}(t) = Au(t) + n(t)$ whose solution is

$$u_i(t) = M(t)u(0) + \int_0^t dt' M(t')n_k(t-t'), \quad (14)$$

where $M(t) = \exp(At)$. According to the Routh-Hurwitz criterion [56], the system reaches around a steady state and stable. i.e; when all the eigenvalues of the coefficient matrix A have negative real parts. As $t \rightarrow \infty$ so that $M(\infty) = 0$ and Eq. (14) can be rewritten as

$$u_i(\infty) = \int_0^\infty dt' \sum_k M(t')n_k(t-t'). \quad (15)$$

Consequently using Eq. (15) we can write $V_{ij} = \frac{1}{2} \langle u_i(\infty)u_j(\infty) + u_j(\infty)u_i(\infty) \rangle$. By using the steady-state solutions in Eqs. (14 - 15) and the fact that the ten components of $n(t)$ are uncorrelated with each other, one gets

$$V_{ij} = \sum_{l,k} \int_0^\infty dt \int_0^\infty dt' M_{ik}(t)M_{jl}(t')n_{kl}(t-t'), \quad (16)$$

where $n_{kl}(t-t') = \frac{1}{2} \langle n_k(t)n_l(t') + n_l(t')n_k(t) \rangle$ is the matrix of stationary noise correlation functions. The Brownian noise term $\xi(t)$ is in general a non-Markovian Gaussian noise, but in the limit of large mechanical quality factor $Q_m = \omega_m/\gamma_m \gg 1$, becomes with a good approximation Markovian [57] with symmetrized correlation function $\langle \xi(t)\xi(t') + \xi(t')\xi(t) \rangle = 2\gamma_m(2n+1)\delta(t-t')$, where $n = [\exp(\frac{\hbar\omega_m}{k_B T}) - 1]^{-1}$ is the mean thermal excitation number of the resonator. As a consequence, $n_{kl}(t-t') = D_{kl}\delta(t-t')$, where $D_{kl} = \text{Diag}[0, \gamma_m(2n+1), \kappa_c, \kappa_c, \kappa_w(2N(\omega_w)+1), \kappa_w(2N(\omega_w)+1), \kappa_a, \kappa_a, \kappa_a, \kappa_a]$ is the diffusion matrix stemming from the noise correlations. So that Eq. (16) becomes

$$V_{ij} = \int_0^\infty ds M_{(s)} D M_{(s)}^T. \quad (17)$$

When the stability condition is fulfilled, the steady-state CM in Eq. (17) is determined by the Lyapunov equation [58]

$$AV + VA^T = -D, \quad (18)$$

which is linear in V and can be straightforwardly solved. However, its explicit solution is cumbersome and will not be reported here. We have five mode Gaussian state characterized by covariance matrix V which can also be expressed in the form of block matrix as:

$$V = \begin{pmatrix} V_m & V_{ma} & V_{mb} & V_{m\sigma_{ba}} & V_{m\sigma_{cb}} \\ V_{ma}^T & V_a & V_{ab} & V_{a\sigma_{ba}} & V_{a\sigma_{cb}} \\ V_{mb}^T & V_{ab}^T & V_b & V_{b\sigma_{ba}} & V_{b\sigma_{cb}} \\ V_{m\sigma_{ba}}^T & V_{a\sigma_{ba}}^T & V_{b\sigma_{ba}}^T & V_{\sigma_{ba}} & V_{\sigma_{ba}\sigma_{cb}} \\ V_{m\sigma_{cb}}^T & V_{a\sigma_{cb}}^T & V_{b\sigma_{cb}}^T & V_{\sigma_{cb}\sigma_{cb}} & V_{\sigma_{cb}} \end{pmatrix}, \quad (19)$$

where each block represents 2×2 matrix. The diagonal blocks show variance within each subsystem, while the off-diagonal blocks shows covariance across different subsystems [59].

4. Opto-electro-mechanical Entanglement Generations

We are interested in the entanglement properties of the steady state of the opto-electro-mechanical system under study. Therefore, we shall focus on the entanglement of the three possible bipartite subsystems. The sub-matrix representing the covariance of the cavity and mechanical subsystem is determined by the first four rows and columns of V . Accordingly, the correlation between an optical cavity-mechanical oscillator (V_s), microwave cavity-mechanical oscillator (V_r), optical cavity-microwave cavity (V_z) subsystem can be represented by:

$$V_s = \begin{pmatrix} V_m & V_{ma} \\ V_{ma}^T & V_a \end{pmatrix}, V_r = \begin{pmatrix} V_m & V_{mb} \\ V_{mb}^T & V_b \end{pmatrix}, V_z = \begin{pmatrix} V_a & V_{ab} \\ V_{ab}^T & V_b \end{pmatrix}, \quad (20)$$

where the index m, a and b represents MR, OC and MC subsystem respectively. The correlation between optical cavity-atom operators are

$$V_t = \begin{pmatrix} V_a & V_{a\sigma_{ba}} \\ V_{a\sigma_{ba}}^T & V_{\sigma_{ba}} \end{pmatrix}, V_y = \begin{pmatrix} V_a & V_{a\sigma_{cb}} \\ V_{a\sigma_{cb}}^T & V_{\sigma_{cb}} \end{pmatrix}, \quad (21)$$

where the index σ_{ba} and σ_{cb} represents atomic operators subsystem. In order to quantify bipartite entanglement among different subsystems, we use logarithmic negativity [60, 61]

$$E_N = \max[0, -\ln 2\eta^-], \quad (22)$$

where $\eta^- = 2^{-\frac{1}{2}} [\Sigma(V_k) - \sqrt{\Sigma(V_k)^2 - 4\det V_k}]^2$ is the lowest symplectic eigenvalue of the partial transpose of the 4×4 CM,

associated with the selected bipartition, obtained by neglecting the rows and columns of the uninteresting mode, where V_k ($k = s, r, z, t, y$) can be expressed in a form of block matrix as Eq. (20) and Eq. (21).

The numerical results of the analysis of bipartite entanglement between subsystems of an opto-electro-mechanical system assisted by a three-level laser. The entanglement properties can be verified by experimentally measuring the corresponding CM through logarithmic negativity. To measure E_N at the steady state, one has to measure all the determined independent entries of the correlation matrix V . We have taken the parameters analogous to the values of the parameter used in experimental work from [62, 52, 63] listed as follow.

The optical cavity length $L = 1 \times 10^{-3} m$, the spacing of capacitor plate $d = 100 \times 10^{-9} m$, permeability $\mu = 0.008$, mechanical resonator mass $m = 10 \times 10^{-12} Kg$, temperature $T = 15 \times 10^{-3} K$, mechanical resonator frequency $\omega_m = 2\pi \times 10^7 Hz$, Microwave cavity frequency $\omega_\omega = 2\pi \times 10^7 Hz$, mechanical quality factor $Q = 5 \times 10^4$, mechanical decay rate $\gamma_m = \omega_m/Q$ with $F = 4.07 \times 10^4$, optical cavity decay rate $\kappa_c = 0.08\omega_m$, microwave cavity decay rate $\kappa_\omega = 0.02\omega_m$, optical cavity detuning $\Delta_w = \omega_m$, optical cavity beam wavelength $\lambda_{oc} = 810 \times 10^{-9} m$, optical cavity beam frequency $\omega_{oc} = 2\pi c/\lambda_{oc}$, optical cavity driven power $P_c = 30 \times 10^{-3} W$, the microwave cavity driven power $P_\omega = 30 \times 10^{-3} W$, and internal energy of the atoms are assumed to be $\rho_{aa}^0 = \rho_{cc}^0 = \rho_{ca}^0 = 0.5$, $\Delta_{a1} = \Delta_{a2} = 2\pi \times 10^7$ are atom transitions detuning respectively

Accordingly, we study the effects of injected atoms on the entanglement between subsystems of the opto-electro-mechanical system and compare it with the standard opto-electromechanical system without three-level of atoms. To this aim, Fig. (2) shows that the plot of logarithmic negativity E_N between OC-MR versus normalized optical cavity detuning Δ_c/ω_m . The red dashed line illustrates the entanglement level within the original OC-MR, whereas the blue dashed line presents the entanglement level of the OC-MR enhanced by a three-level laser. By introducing three-level atoms into the opto-electro-mechanical system, higher degrees of entanglement can be achieved due to the added three level laser-field interaction. In this case, the entanglement between the optical and mechanical components can be improved by the atomic degree of freedom. This enhancement enables more robust and efficient entanglement generation and more control over the entangled state.

In Fig. (3), we can see two different entanglement scenarios regarding the interaction between an MC-MR, one without the injection of a three-level atom (red dashed line) and one where a three-level atom is injected into the cavity (blue dashed line). In the first scenario (red dashed line), the entanglement between MC-MR is generated solely from the interaction between the two subsystems without atom injection. This curve thus depicts the baseline level of entanglement generated by the interaction of the two subsystems. The entanglement arises due to the radiation pressure of the optical cavity on the MR, which results in a change in the length of the capacitor connecting the two subsystems. On the other hand, the blue dashed line represents the

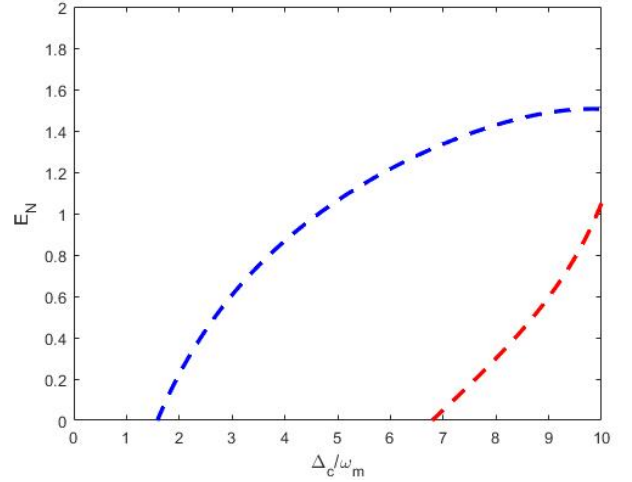


Figure 2: The plot of logarithmic negativity E_N between OC-MR versus normalized optical cavity detuning Δ_c/ω_m , with out injection of atom (red line) and with injection of atom (blue line), the parameters we used are $L = 1 \times 10^{-3} m$, $d = 100 \times 10^{-9} m$, $\mu = 0.008$, $m = 10 \times 10^{-12} Kg$, $T = 15 \times 10^{-3} K$, $\omega_m = 2\pi \times 10^7 Hz$, $\omega_\omega = 2\pi \times 10^7 Hz$, $\gamma_m = 200\pi$, $\kappa_c = 0.1\omega_m$, $\kappa_w = 0.08\omega_m$, $\Delta_w = \omega_m$, $\lambda_{oc} = 810 \times 10^{-9} m$, $\omega_{oc} = 2\pi c/\lambda_{oc}$, $P_c = 30 \times 10^{-3} W$, $P_\omega = 30 \times 10^{-3} W$, $r_a = 1.6 \times 10^5$, $g = 2\pi \times 8 \times 10^5$, $\Delta_{a1} = 2\pi \times 10^{10}$, $\Delta_{a2} = 2\pi \times 10^7$, $\rho_{aa}^0 = \rho_{cc}^0 = \rho_{ca}^0 = 0.5$, the other parametres are listed in main text.

entanglement between the MC-MR when a three-level atom is injected into the optical cavity at the rate r_a . By comparing the red and blue dashed lines, one can observe that the presence of a three-level laser indeed enhances the entanglement between the MC-MR, especially for specific values of the normalized detuning parameter, Δ_c/ω_m .

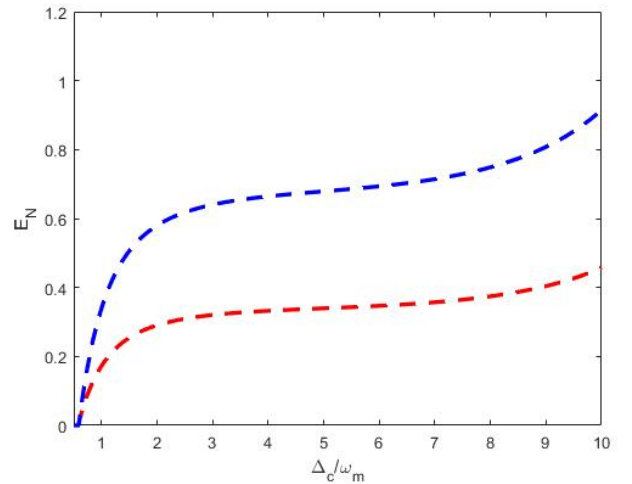


Figure 3: The plot of logarithmic negativity E_N between MC-MR versus normalize optical cavity detuning Δ_c/ω_m , without injection of atom (red line) and with injection of atom (blue line), the parameters we used are $\kappa_c = 0.08\omega_m$, $r_a = 2000$, $\Delta_{a1} = \Delta_{a2} = 2\pi \times 10^7$, $\gamma_m = \omega_m/Q$, $g = 2\pi \times 1.0 \times 10^5$, $\kappa_a = 2\pi \times 10^5$, $\Delta_w = \omega_m$ and the others parameters are the same as Fig. (2).

Fig. (4) illustrates an entanglement setup involving OC-MC

subsystems. In this case, the red dashed line represents the entanglement between the optical and microwave cavities. In contrast, the blue dashed line signifies the entanglement between OC-MC, with the three-level atom being injected into the optical cavity at a rate of r_a . It is essential to highlight that the entanglement between OC-MC is not achieved through direct interaction but is mediated by the mechanical resonator.

On the other hand, the blue dashed line represents the entanglement between OC-MC when the three-level laser is present. As the atom is injected into the OC, the emitted laser experiences a coupling between the optical cavity field mode. This coupling induces an indirect interaction between the OC-MC, promoting entanglement generation. When we compare the two situations, it is clear that the presence of the three-level laser significantly improves the entanglement between the optical and microwave cavities. This suggests that the injection of the atom alters the dynamics of the OC, MC, and MR system, which leads to the enhancement of the entanglement process. Moreover, by controlling the injection rate, the level of entanglement can be adjusted according to desired parameters.

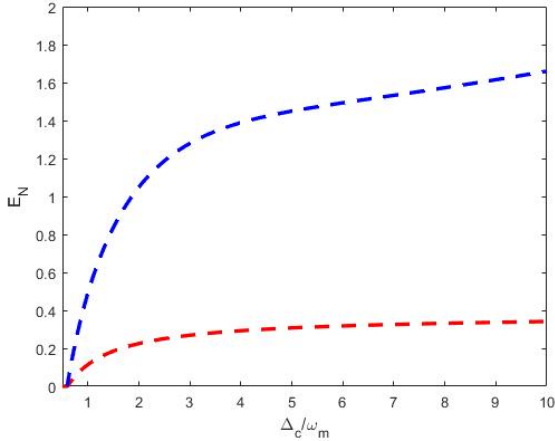


Figure 4: The plot of logarithmic negativity E_N between OC-MC versus normalized optical cavity detuning Δ_c/ω_m , without injection of atom (red line) and with injection of atom (blue line), the parameters we used are $r_a = 1.6 \times 10^6$, $\Delta_{a1} = 2\pi \times 10^{10}$, $\Delta_{a2} = 2\pi \times 10^6$, $g = 2\pi \times 1.5 \times 10^6$, $\kappa_c = 0.08\omega_m$ and the others parameters are the same as Fig. (2).

The inclusion of a three-level laser can also increase the system's coherence and stability, which in turn can improve performance in a range of quantum applications like quantum information processing and communication, where robust entanglement between quantum systems is desirable. In general, in the above three bipartite entanglement between subsystems OC-MR, OC-MC, and MR-MC, it is shown that the subsystem containing OC has higher logarithmic negativity due to the atom injected into the optomechanical arrangement and emitted laser, which interact with OC. Also, it is shown that the entanglement between subsystems of the opto-electro-mechanical system discussed above is indeed enhanced compared to the entanglement of opto-electro-mechanical studied by [40, 34].

Fig. (5) is a plot of logarithmic negativity E_N between

OC-three level laser against normalized optical cavity detuning Δ_c/κ_c for different three-level laser-cavity field coupling rates g . Three scenarios are presented in the plot, distinguished by different colored solid lines. The purpose of these three scenarios is to demonstrate how the entanglement between the optical cavity and three level laser varies as the coupling rate is increased. As the coupling rate increases, represented by the

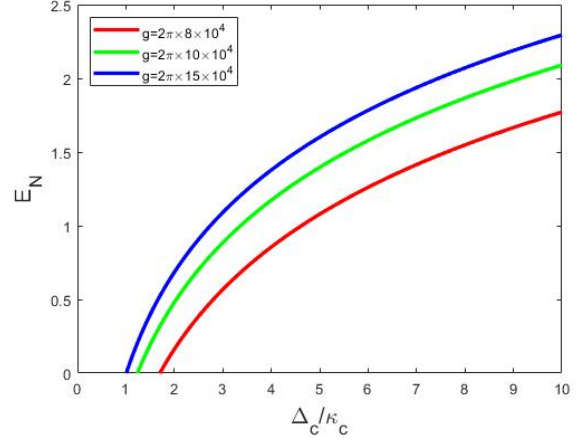


Figure 5: The plot of logarithmic negativity E_N between OC-three level laser versus normalized optical cavity detuning Δ_c/κ_c at different three-level laser-cavity field coupling rate, the parameters we used are $r_a = 1.6 \times 10^6$, $\Delta_{a1} = \Delta_{a2} = 2\pi \times 10^6$, $\kappa_a = 2\pi \times 10^5$, $\kappa_c = 0.02$ and the others parameters are the same as Fig. (2).

color change from red to blue, the entanglement (logarithmic negativity) also increases. This implies that the degree of correlation between the two subsystems, the optical cavity, and three-level lasers, becomes stronger as the three-level laser-cavity field coupling rate is increased [64]. Furthermore, the dependence of logarithmic negativity on the normalized optical cavity detuning (Δ_c/κ_c) can be observed as well. The entanglement increases as the detuning is increased but reaches a peak at a particular value of Δ_c/κ_c and then starts to decrease. This shows an optimal detuning value that maximizes the entanglement between the optical cavity and three-level laser for a given coupling rate. The peak entanglement value, i.e., the maximum logarithmic negativity and the optimal detuning value at which this maximum entanglement occurs, increases as the coupling rate increases.

As shown in Fig. (6), the logarithmic negativity E_N for three bipartite entanglement versus the normalized optical cavity detuning Δ_c/ω_m at three different temperatures. The first sub-plot (a) shows the logarithmic negativity for three bipartite entanglements versus the normalized optical cavity detuning Δ_c/ω_m at temperature $T = 5 \times 10^{-3} K$. It can be observed that the entanglement between OC-MC is higher compared to others. The second sub-plot (b) shows the logarithmic negativity for three bipartite entanglement versus the normalized optical cavity detuning Δ_c/ω_m at temperature $T = 250 \times 10^{-3} K$. We can see that the entanglement between each subsystem begins to decrease as temperature increases. Finally, the third sub-plot (c)

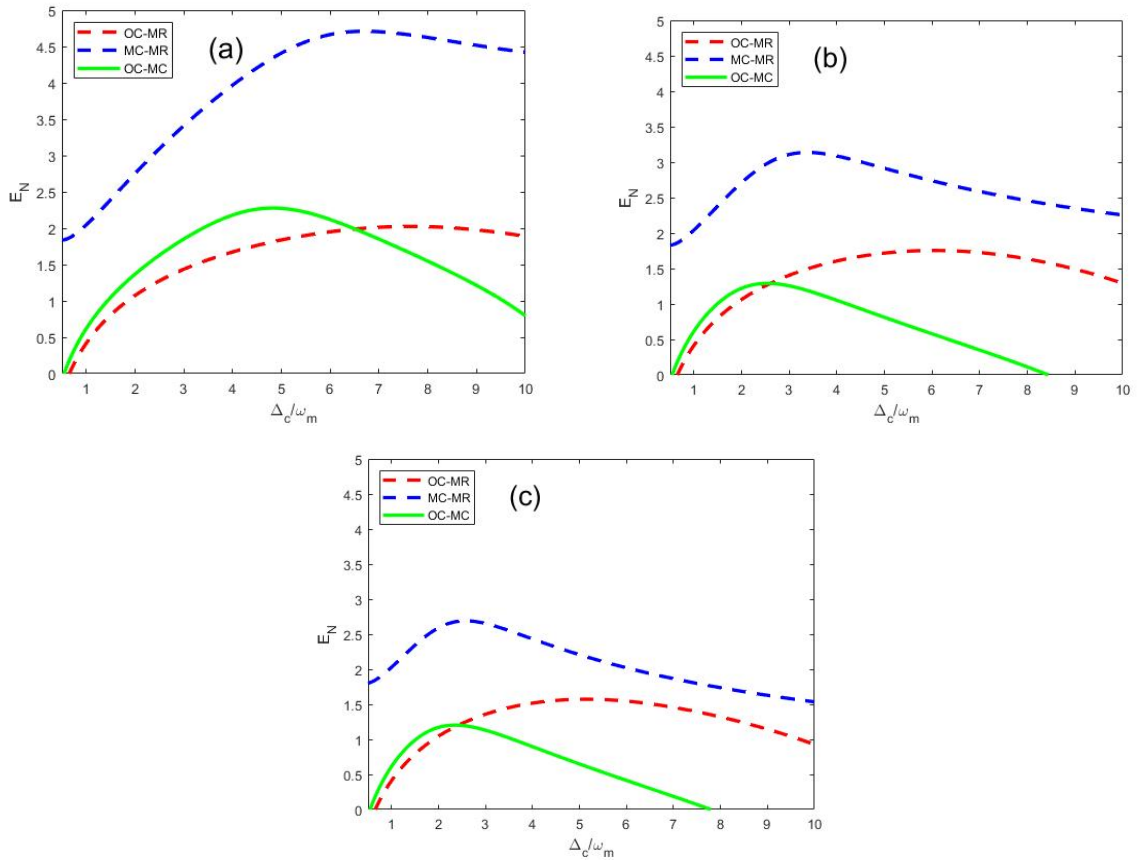


Figure 6: The plot of E_N of the three bipartite sub-systems versus the normalized optical cavity detuning Δ_c/ω_m at three different temperatures: $T = 5 \times 10^{-3} K$ (a), $T = 250 \times 10^{-3} K$ (b), $T = 350 \times 10^{-3} K$ (c), the parameters we used are $r_a = 1.6 \times 10^6$, $\Delta_{a1} = 2\pi \times 10^{10}$, $\Delta_{a2} = 2\pi \times 10^6$, $\gamma_m = 200\pi$, $F = 4.07 \times 10^4$, $\kappa_c = \pi c/(F \times L)$, $g = 2\pi \times 1.0 \times 10^5$, $\kappa_a = 2\pi \times 10^6$, $\Delta_w = -\omega_m$ and the others parameters are the same as Fig. (2).

presents logarithmic negativity for three bipartite entanglement versus the normalized optical cavity detuning Δ_c/ω_m at temperature $T = 350 \times 10^{-3} K$. Different colored lines represent the entanglement between the different subsystems. From this, it can be observed that the entanglement between each subsystem decreases as the temperature increases from $T = 5 \times 10^{-3} K$ (a) to $T = 350 \times 10^{-3} K$ (c). This can be attributed to the fact that entanglement is a quantum mechanical property that tends to become fragile with increasing temperature [57]. As the environment becomes warmer, the increased thermal fluctuations lead to greater decoherence and noise, negatively impacting the entanglement between the various subsystems.

Additionally, by altering the parameter, one can control the level of entanglement in the system. This entanglement tunability may have implications for designing robust entangled systems for various practical applications. Moreover, this relationship may indicate that the behavior of the entangled subsystem pairs is sensitive to temperature, with higher temperatures leading to decay entanglement between the subsystems. When we compare the peaks of the plotted lines for each temperature, it is evident that the entanglement between the OC-MC pair significantly decays at higher temperatures than the entanglement in the OC-MR and MC-MR pairs. This is because the entanglement between OC-MC is increased due to the OC-MR and

MC-MR entanglement.

5. Conclusion

In conclusion, the study focused on improving bipartite entanglement in an opto-electro-mechanical system utilizing three-level atoms. A system's dynamics have been studied using the QLEs and linearization approximation, leading to a correlation matrix containing block matrices describing entanglement between each subsystem. Accordingly, the bipartite entanglement is quantified through logarithmic negativity. Specifically, we investigate the entanglement properties generated between various subsystems, including the OC-MC, OC-MR, and MC-MR subsystems. The numerical results indicated that introducing three-level atoms into opto-electro-mechanical systems significantly enhances the entanglement between each subsystem. In addition, we showed that the degree of correlation between the optical cavity and three-level lasers becomes stronger as the three-level laser-cavity field coupling rate increases. A higher coupling rate allows for faster and more reliable information exchange, enabling efficient communication and synchronization between different system parts. Moreover, the results demonstrated that temperature has a significant impact on entanglement, with higher temperatures leading to a

reduction in entanglement between the subsystems. This increased interaction leads to a decrease in entanglement between the subsystems as their states become more independent due to the influence of the environment.

References

- [1] M. Aspelmeyer, T. J. Kippenberg, F. Marquardt, Cavity optomechanics, *Reviews of Modern Physics* 86 (4) (2014) 1391.
- [2] T. J. Kippenberg, K. J. Vahala, Cavity optomechanics: back-action at the mesoscale, *science* 321 (5893) (2008) 1172–1176.
- [3] D.-Y. Wang, C.-H. Bai, S. Liu, S. Zhang, H.-F. Wang, Optomechanical cooling beyond the quantum backaction limit with frequency modulation, *Physical Review A* 98 (2) (2018) 023816.
- [4] J. Chan, T. M. Alegre, A. H. Safavi-Naeini, J. T. Hill, A. Krause, S. Gröblacher, M. Aspelmeyer, O. Painter, Laser cooling of a nanomechanical oscillator into its quantum ground state, *Nature* 478 (7367) (2011) 89–92.
- [5] V. Singh, S. Bosman, B. Schneider, Y. M. Blanter, A. Castellanos-Gomez, G. Steele, Optomechanical coupling between a multilayer graphene mechanical resonator and a superconducting microwave cavity, *Nature nanotechnology* 9 (10) (2014) 820–824.
- [6] A. H. Safavi-Naeini, J. Chan, J. T. Hill, T. P. M. Alegre, A. Krause, O. Painter, Observation of quantum motion of a nanomechanical resonator, *Physical Review Letters* 108 (3) (2012) 033602.
- [7] A. Jöckel, A. Faber, T. Kampschulte, M. Korppi, M. T. Rakher, P. Treutlein, Sympathetic cooling of a membrane oscillator in a hybrid mechanical–atomic system, *Nature nanotechnology* 10 (1) (2015) 55–59.
- [8] S. Mancini, D. Vitali, P. Tombesi, Optomechanical cooling of a macroscopic oscillator by homodyne feedback, *Physical Review Letters* 80 (4) (1998) 688.
- [9] J. M. Dobrindt, I. Wilson-Rae, T. J. Kippenberg, Parametric normal-mode splitting in cavity optomechanics, *Physical Review Letters* 101 (26) (2008) 263602.
- [10] T. P. Purdy, P.-L. Yu, R. W. Peterson, N. S. Kampel, C. A. Regal, Strong optomechanical squeezing of light, *Physical Review X* 3 (3) (2013) 031012.
- [11] R. Ghobadi, S. Kumar, B. Pepper, D. Bouwmeester, A. Lvovsky, C. Simon, Optomechanical micro-macro entanglement, *Physical Review Letters* 112 (8) (2014) 080503.
- [12] H. Flayac, M. Minkov, V. Savona, Remote macroscopic entanglement on a photonic crystal architecture, *Physical Review A* 92 (4) (2015) 043812.
- [13] B. Teklu, T. Byrnes, F. S. Khan, Cavity-induced mirror-mirror entanglement in a single-atom raman laser, *Phys. Rev. A* 97 (2018) 023829.
- [14] H. D. Mekonnen, T. G. Tesfahannes, T. Y. Darge, S. Eshete, Boosting macroscopic entanglement in charged cavity optomechanical system through coherent feedback loop, *Journal of Optics* (2024) 1–9.
- [15] T. P. Purdy, R. W. Peterson, C. Regal, Observation of radiation pressure shot noise on a macroscopic object, *Science* 339 (6121) (2013) 801–804.
- [16] V. Montenegro, M. G. Genoni, A. Bayat, M. G. A. Paris, Mechanical oscillator thermometry in the nonlinear optomechanical regime, *Phys. Rev. Res.* 2 (2020) 043338.
- [17] V. Montenegro, M. G. Genoni, A. Bayat, M. G. A. Paris, Probing of nonlinear hybrid optomechanical systems via partial accessibility, *Phys. Rev. Res.* 4 (2022) 033036.
- [18] M. Asjad, B. Teklu, M. G. A. Paris, Joint quantum estimation of loss and nonlinearity in driven-dissipative kerr resonators, *Phys. Rev. Res.* 5 (2023) 013185.
- [19] V. Fiore, Y. Yang, M. C. Kuzyk, R. Barbour, L. Tian, H. Wang, Storing optical information as a mechanical excitation in a silica optomechanical resonator, *Physical review letters* 107 (13) (2011) 133601.
- [20] K. Stannigel, P. Komar, S. Habraken, S. Bennett, M. D. Lukin, P. Zoller, P. Rabl, Optomechanical quantum information processing with photons and phonons, *Physical review letters* 109 (1) (2012) 013603.
- [21] C. H. Bennett, G. Brassard, C. Crépeau, R. Jozsa, A. Peres, W. K. Wootters, Teleporting an unknown quantum state via dual classical and einstein-podolsky-rosen channels, *Physical review letters* 70 (13) (1993) 1895.
- [22] A. K. Ekert, Quantum cryptography based on bell’s theorem, *Physical review letters* 67 (6) (1991) 661.
- [23] M. Lu, Y. Xia, L.-T. Shen, J. Song, N. B. An, Shortcuts to adiabatic passage for population transfer and maximum entanglement creation between two atoms in a cavity, *Physical Review A* 89 (1) (2014) 012326.
- [24] C. H. Bennett, S. J. Wiesner, Communication via one-and two-particle operators on einstein-podolsky-rosen states, *Physical review letters* 69 (20) (1992) 2881.
- [25] Y. Xia, H.-S. Song, Controlled quantum secure direct communication using a non-symmetric quantum channel with quantum superdense coding, *Physics Letters A* 364 (2) (2007) 117–122.
- [26] A.-D. Zhu, Y. Xia, Q.-B. Fan, S. Zhang, Secure direct communication based on secret transmitting order of particles, *Physical Review A* 73 (2) (2006) 022338.
- [27] F.-G. Deng, X.-H. Li, C.-Y. Li, P. Zhou, H.-Y. Zhou, Multiparty quantum-state sharing of an arbitrary two-particle state with einstein-podolsky-rosen pairs, *Physical Review A* 72 (4) (2005) 044301.
- [28] Y.-D. Wang, A. A. Clerk, Reservoir-engineered entanglement in optomechanical systems, *Physical review letters* 110 (25) (2013) 253601.
- [29] C. Dong, V. Fiore, M. C. Kuzyk, H. Wang, Optomechanical dark mode, *Science* 338 (6114) (2012) 1609–1613.
- [30] T. Gebremariam, Y.-X. Zeng, M. Mazaheri, C. Li, Enhancing optomechanical force sensing via precooling and quantum noise cancellation, *Science China Physics, Mechanics & Astronomy* 63 (2020) 1–11.
- [31] J. T. Hill, A. H. Safavi-Naeini, J. Chan, O. Painter, Coherent optical wavelength conversion via cavity optomechanics, *Nature communications* 3 (1) (2012) 1196.
- [32] F. Massel, S. U. Cho, J.-M. Pirkkalainen, P. J. Hakonen, T. T. Heikkilä, M. A. Sillanpää, Multimode circuit optomechanics near the quantum limit, *Nature communications* 3 (1) (2012) 987.
- [33] B. Xiong, X. Li, X.-Y. Wang, L. Zhou, Improve microwave quantum illumination via optical parametric amplifier, *Annals of Physics* 385 (2017) 757–768.
- [34] S. Barzanjeh, D. Vitali, P. Tombesi, G. Milburn, Entangling optical and microwave cavity modes by means of a nanomechanical resonator, *Physical Review A* 84 (4) (2011) 042342.
- [35] F. Eftekhari, M. Tavassoly, A. Behjat, Nonlinear interaction of a three-level atom with a two-mode field in an optomechanical cavity: Field and mechanical mode dissipations, *Physica A: Statistical Mechanics and its Applications* 596 (2022) 127176.
- [36] L. Midolo, A. Schliesser, A. Fiore, Nano-opto-electro-mechanical systems, *Nature nanotechnology* 13 (1) (2018) 11–18.
- [37] T. Gebremariam, M. Mazaheri, Y. Zeng, C. Li, Dynamical quantum steering in a pulsed hybrid opto-electro-mechanical system, *JOSA B* 36 (2) (2019) 168–177.
- [38] J. Li, S. Gröblacher, Stationary quantum entanglement between a massive mechanical membrane and a low frequency lc circuit, *New Journal of Physics* 22 (6) (2020) 063041.
- [39] D. Cattiaux, X. Zhou, S. Kumar, I. Golokolenov, R. Gazizulin, A. Luck, L. M. de Lépinay, M. Sillanpää, A. Armour, A. Fefferman, et al., Beyond linear coupling in microwave optomechanics, *Physical Review Research* 2 (3) (2020) 033480.
- [40] T. G. Tesfahannes, D. Alemu, Stationary entanglement dynamics in a hybrid opto-electro-mechanical system, *Romanian Journal of Physics* 66 (3-4) (2021).
- [41] H. D. Mekonnen, T. G. Tesfahannes, T. Y. Darge, A. G. Kumela, Quantum correlation in a nano-electro-optomechanical system enhanced by an optical parametric amplifier and coulomb-type interaction, *Scientific Reports* 13 (1) (2023) 13800.
- [42] J. Wang, X.-D. Tian, Y.-M. Liu, C.-L. Cui, J.-H. Wu, Entanglement manipulation via coulomb interaction in an optomechanical cavity assisted by two-level cold atoms, *Laser Physics* 28 (6) (2018) 065202.
- [43] B. Teklu, Continuous-variable entanglement dynamics in lorentzian environment, *Physics Letters A* 432 (2022) 128022.
- [44] B. Teklu, M. Bina, M. G. A. Paris, Noisy propagation of gaussian states in optical media with finite bandwidth, *Scientific Reports* 12 (1) (2022) 11646.
- [45] E. Mosisa, Enhanced squeezing and entanglement in nondegenerate three-level laser coupled to squeezed vacuum reservoir, *Advances in Mathematical Physics* 2021 (2021) 1–12.
- [46] D. Vitali, P. Tombesi, M. Woolley, A. Doherty, G. Milburn, Entangling a nanomechanical resonator and a superconducting microwave cavity, *Physical Review A* 76 (4) (2007) 042336.

- [47] M. Wang, X.-Y. Lü, J.-Y. Ma, H. Xiong, L.-G. Si, Y. Wu, Controllable chaos in hybrid electro-optomechanical systems, *Scientific reports* 6 (1) (2016) 22705.
- [48] Q. Cai, J. Liao, Q. Zhou, Entangling two microwave modes via optomechanics, *Physical Review A* 100 (4) (2019) 042330.
- [49] Y. Li, L. Deng, T. Yin, A. Chen, Entanglement between two mechanical oscillators in a dual-coupling optomechanical system, *Frontiers in Physics* 10 (2022) 908205.
- [50] M. Abdi, S. Barzanjeh, P. Tombesi, D. Vitali, Effect of phase noise on the generation of stationary entanglement in cavity optomechanics, *Physical Review A* 84 (3) (2011) 032325.
- [51] C. Gardiner, P. Zoller, *Quantum noise: a handbook of Markovian and non-Markovian quantum stochastic methods with applications to quantum optics*, Springer Science & Business Media, 2004.
- [52] L. Zhou, Y. Han, J. Jing, W. Zhang, Entanglement of nanomechanical oscillators and two-mode fields induced by atomic coherence, *Physical Review A* 83 (5) (2011) 052117.
- [53] T. G. Tesfahannes, Generation of the bipartite entanglement and correlations in an optomechanical array, *JOSA B* 37 (11) (2020) A245–A252.
- [54] C. Jiang, H. Lu, Z. Zhai, G. Chen, Phase-controlled entanglement in a four-mode optomechanical system, in: *Photonics*, Vol. 9, MDPI, 2022, p. 818.
- [55] Y.-F. Jiao, J.-X. Liu, Y. Li, R. Yang, L.-M. Kuang, H. Jing, Nonreciprocal enhancement of remote entanglement between nonidentical mechanical oscillators, *Physical Review Applied* 18 (6) (2022) 064008.
- [56] M. Schumacher, *Stability and entanglement in an optomechanical system*, Rochester Institute of Technology, 2013.
- [57] C. Genes, A. Mari, P. Tombesi, D. Vitali, Robust entanglement of a micromechanical resonator with output optical fields, *Physical Review A* 78 (3) (2008) 032316.
- [58] C. Genes, D. Vitali, P. Tombesi, Emergence of atom-light-mirror entanglement inside an optical cavity, *Physical Review A* 77 (5) (2008) 050307.
- [59] C.-H. Bai, D.-Y. Wang, H.-F. Wang, A.-D. Zhu, S. Zhang, Robust entanglement between a movable mirror and atomic ensemble and entanglement transfer in coupled optomechanical system, *Scientific reports* 6 (1) (2016) 33404.
- [60] G. Vidal, R. F. Werner, Computable measure of entanglement, *Phys. Rev. A* 65 (2002) 032314.
- [61] M. B. Plenio, Logarithmic negativity: A full entanglement monotone that is not convex, *Phys. Rev. Lett.* 95 (2005) 090503.
- [62] J. D. Teufel, D. Li, M. Allman, K. Cicak, A. Sirois, J. Whittaker, R. Simmonds, Circuit cavity electromechanics in the strong-coupling regime, *Nature* 471 (7337) (2011) 204–208.
- [63] S. Barzanjeh, M. Abdi, G. J. Milburn, P. Tombesi, D. Vitali, Reversible optical-to-microwave quantum interface, *Physical Review Letters* 109 (13) (2012) 130503.
- [64] D. J. Gelmecha, A. Sohail, J. Peng, A. Shahzad, J.-X. Peng, T. Abebe, Controllable fano-type optical response and four-wave mixing via magnetoelastic coupling in amagno (opto) mechanical system, Available at SSRN 4169734.